JACS
JOURNAL OF THE AMERICAN CHEMICAL SOCIETY
Communication
pubs.acs.org/JACS

Iron Complexes of Square Planar Tetradentate Polypyridyl-Type Ligands as Catalysts for Water Oxidation

Lanka D. Wickramasinghe,[†] Rongwei Zhou,[†] Ruifa Zong,[†] Pascal Vo,[†] Kevin J. Gagnon,[‡] and Randolph P. Thummel*[,†]

[†]Department of Chemistry, 112 Fleming Building, University of Houston, Houston, Texas 77204-5003, United States
[‡]Advanced Light Source, Lawrence Berkeley National Lab, 1 Cyclotron Rd., Berkeley, California 94720, United States

Supporting Information

ABSTRACT: The tetradentate ligand, 2-(pyrid-2′-yl)-8-(1″,10″-phenanthrolin-2″-yl)-quinoline (ppq) embodies a quaterpyridine backbone but with the quinoline C8 providing an additional sp^2 center separating the two bipyridine-like subunits. Thus, the four pyridine rings of ppq present a neutral, square planar host that is well suited to first-row transition metals. When reacted with $FeCl_3$, a μ-oxo-bridged dimer is formed having a water bound to an axial metal site. A similar metal-binding environment is presented by a bis-phenanthroline amine (dpa) which forms a 1:1 complex with $FeCl_3$. Both structures are verified by X-ray analysis. While the Fe^{III}(dpa) complex shows two reversible one-electron oxidation waves, the Fe^{III}(ppq) complex shows a clear two-electron oxidation associated with the process $H_2O{-}Fe^{III}Fe^{III} \rightarrow H_2O{-}Fe^{IV}Fe^{IV} \rightarrow O{=}Fe^{V}Fe^{III}$. Subsequent disproportionation to an Fe=O species is suggested. When the Fe^{III}(ppq) complex is exposed to a large excess of the sacrificial electron-acceptor ceric ammonium nitrate at pH 1, copious amounts of oxygen are evolved immediately with a turnover frequency (TOF) = 7920 h^{-1}. Under the same conditions the mononuclear Fe^{III}(dpa) complex also evolves oxygen with TOF = 842 h^{-1}.

As the world's economies expand and the global demands for energy increase, a strong mandate has emerged for a shift away from fossil-based fuels to a hydrogen-based economy. The ideal source for the massive amounts of hydrogen that will be needed is water, and thus the realization of solar energy promoted decomposition of water into its elements has become a Holy Grail for the 21st century. A significant breakthrough in this area occurred about 10 years ago with the discovery that mononuclear Ru^{II} complexes could catalyze the oxidation of water in the presence of a sacrificial chemical oxidant.[1] Because of the attractive electro- and photochemical properties of its polypyridyl complexes, Ru^{II} was initially the metal of choice for water oxidation studies and very soon a variety of catalysts based on this metal were reported.[2] The fact that complexes of Ru^{II} are air-stable, diamagnetic with well-behaved redox properties and absorption/emission behavior made them ideal choices for initial water decomposition studies. More recently, as the field progressed, the demand for catalysts based on more economically feasible, earth-abundant first-row transition metals began to increase. Situated just above ruthenium on the periodic chart, iron became a target for oxidation catalyst design. This approach is given further impetus by the fact that iron acts as an important oxygen-transfer agent in physiological respiration.

Several different types of ligands have been used to form iron-based water oxidation catalysts. Collins et al. reported on a series of Fe complexes with tetraamido macrocyclic ligands.[3] It was suggested that these catalysts might involve an $Fe^{V}{=}O$ intermediate.[4] Although several of these systems were quite active, unfortunately this activity was rather short-lived. A recent study on the Fe^{III} complex of *N*,*N*-dimethyl-2,11-diaza[3,3]-(2,6)pyridinophane shows good water oxidation activity and suggests the involvement of $Fe^{IV}{=}O$ or $Fe^{V}{=}O$ intermediates.[5]

Other nonmacrocyclic pyridine-containing tetra- and pentadentate ligands provided Fe complexes that showed modest water oxidation activity.[6] In several cases a quinoline moiety was incorporated into the ligand backbone.[7] It was suggested by Costas et al. that iron complexes having cis-oriented labile sites were more active than similar complexes with trans-oriented labile sites.[8] Several different groups have reported on the unusual reactivity of μ-oxo bridged dinuclear iron complexes[9] especially in water oxidation.[10] Lau et al. have suggested that at low pH multidentate N-donor iron complexes accomplish water oxidation through a molecular iron-oxo intermediate.[11] At high pH, however, they claim that ligand dissociation occurs to generate Fe_2O_3 nanoparticles that catalyze water oxidation.

Recently we reported a new tetradentate polypyridine ligand, 2-(pyrid-2′-yl)-8-(1″,10″-phenanthrolin-2″-yl)-quinoline (ppq) that embodies a quaterpyridine backbone but with the quinoline C8 providing an additional sp^2 center separating the two bipyridine-like subunits.[12] The result is a more square planar arrangement of the four pyridine binding units. The smaller first-row transition metal Co^{II} readily formed a complex with ppq that demonstrated a comfortable 5-6-5 chelate ring pattern. We found that in the presence of $[Ru(bpy)_3]Cl_2$, ascorbic acid and a blue LED at pH = 4.5, the Co-ppq complex was an excellent proton reduction catalyst.[12]

An impediment to the study of complexes based on ppq is the difficulty in accessing 2-nitro-3-bromobenzaldehyde which is reduced to the corresponding amine and then used in the initial Friedländer condensation to afford 8-bromo-2-(pyrid-2′-yl)-quinoline (**4**). We have developed a four-step alternate synthesis of **4** starting with the amide **1** derived from the reaction of 2-

Received: August 26, 2015
Published: October 1, 2015

DOI: 10.1021/jacs.5b08856
J. Am. Chem. Soc. 2015, 137, 13260−13263

bromoaniline and cinnamoyl chloride[13] (Scheme 1). This material undergoes an intramolecular Friedel–Crafts acylation

Scheme 1

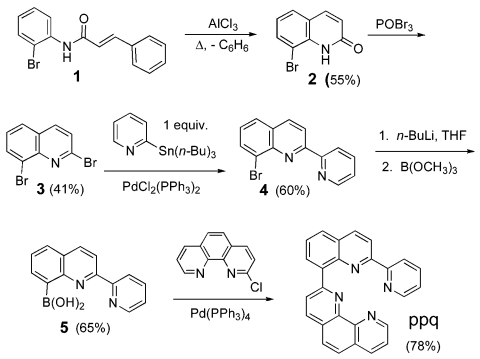

followed by the thermal loss of benzene to give the bromoquinolone **2**. Treatment of this material with $POBr_3$ gives **3**.[14] The Stille coupling of **3** with 2-pyridyl-tri-*n*-butylstannane occurs selectively at the 2-position to provide **4**. In the final step, we have replaced the Friedländer condensation with a Suzuki coupling of **5** with 2-chloro-1,10-phenanthroline to afford ppq in 78% yield.

The geometry of ppq is rather unique in that the binding cavity, in its all-cisoid conformation, involves four pyridine rings in a square planar arrangement. In surveying the literature, we find only a very few systems with a similar geometry. These are mainly bis-phenanthrolines linked at their 2-position with either a carbonyl group[15] or a tertiary amine. Following a reported procedure, we prepared the known diphen amine (dpa)[16] in order to compare its metal binding properties to ppq. When a CH_2Cl_2 solution of either ppq or dpa was treated with a MeOH solution of $FeCl_3$, a complex readily formed (Scheme 2) and was

Scheme 2

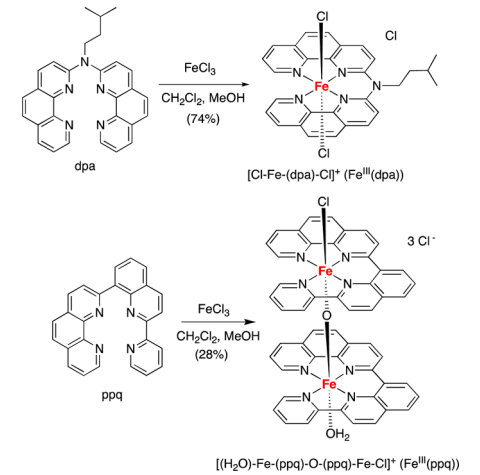

characterized by X-ray crystallography. Interestingly, while dpa formed a 1:1 complex with $FeCl_3$, ppq formed a μ-oxo-bridged dimer (Figure 1). Pertinent bond lengths and bond angles are summarized in Table S2.

Several interesting geometric features for the two complexes can be pointed out (Table S2). The Fe–N bond lengths fall into a rather narrow range for each complex. For the ppq complex they are slightly longer at 2.11–2.16 Å, while for the dpa complex

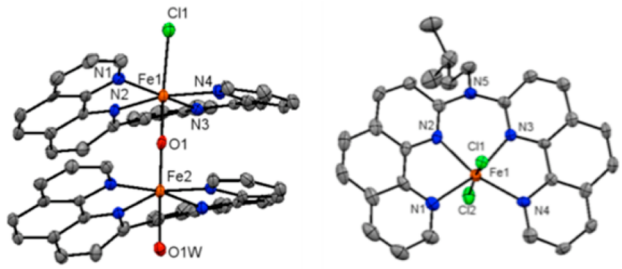

Figure 1. X-ray crystal structure of Fe^{III}(ppq) (left) and Fe^{III}(dpa) (right) showing ellipsoids at 50% probability "with hydrogens, unbound water molecules, and unbound ions omitted for clarity.

they are 2.09–2.11 Å. The Fe–Cl bond for the ppq complex is 0.11–0.15 Å longer than the Fe–Cl bonds in the dpa complex. This increased Fe–Cl bond length implies more polar bonds that are more easily broken. For the ppq complex the interior Fe–O bonds are 0.38–0.35 Å shorter than the exterior Fe–OH_2 bond. The five-membered chelate rings have N–Fe–N angles that are more acute at 78.4–79.9 Å, while the N–Fe–N angles for the six-membered chelate ring are closer to the ideal 90° at 85.3°, 87.8°, and 88.0°. The exterior N–Fe–N angle is considerably expanded at 112.1–115.6°. All these data support the fact that the complexes have rather similar geometries. We suspect that it is the *N*-isopentyl group in the dpa complex that may inhibit formation of a μ-oxo-bridged dimer.

The electrochemical behavior of both Fe complexes was measured in CH_3CN, and the results are recorded in Table 1 and

Table 1. Cyclic Voltammetry Data for Fe^{III} Complexes[a]

complex	$E_{1/2}$, (ΔE_p) (V)	$E_{1/2}$, (ΔE_p) (V)	$E_{1/2}$, (ΔE_p) (V)
Fe^{III}(ppq)	−0.87 (62 mV)	0.01 (75 mV)	0.49 (55 mV)
Fe^{III}(dpa)	−1.20 (94 mV)	0.01 (76 mV)	0.45 (86 mV)

[a]Measured in CH_3CN with carbon working electrode, Pt auxiliary electrode, and Ag/AgCl reference electrode at a scan rate of 100 mV/s with $TBAPF_6$ as the supporting electrolyte.

illustrated in Figure 2. Fe^{III}(ppq) showed a reversible oxidation at 0.01 V (ΔE_p = 75 mV) and another quasi-reversible oxidation at 0.49 V (ΔE_p = 55 mV) vs Ag/AgCl. The current amplitude observed for the first oxidation is more than twice as great as that observed for the second oxidation process, suggesting that the first oxidation is likely a two-electron process. This process can be tentatively attributed to the simultaneous oxidation of the two Fe^{III}-centers ($Fe^{III}Fe^{III} \rightarrow Fe^{IV}Fe^{IV}$). The observation of a single two-electron wave can be explained in two ways. In one case the two Fe centers do not interact at all and thus both oxidize at the same potential, but this explanation seems unlikely since the two Fe centers are separated by only one atom. More likely, the Fe^{III}(ppq) core (Cl-Fe^{III}(ppq)-O-Fe^{III}(ppq)-OH_2) could behave as a single species and undergo a two-electron oxidation. This explanation would agree with electrochemical theory which states that the current passed for a one-electron process (A) is equal to $n^{1/2}$ which equals 1.0 when n = 1. Similarly, the current passed for a two-electron process (B) is equal to $n^{3/2}$ which is 2.82 for n = 2.[17] The B/A ratio from Figure 2 is 2.71. The direct two-electron oxidation would afford a $Fe^{IV}Fe^{IV}$–OH_2 species that could then disproportionate with the loss of two protons to afford a $Fe^{III}Fe^{V}$=O species. The oxidation process observed at 1.3 V was confirmed as the oxidation of chloride by the enhancement of this wave upon the addition of KCl (Figure S1).

DOI: 10.1021/jacs.5b08856
J. Am. Chem. Soc. 2015, 137, 13260–13263

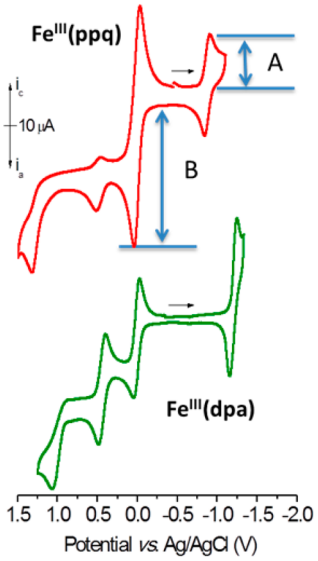

Figure 2. Cyclic voltammetry data of Fe^{III} complexes measured in CH_3CN with carbon working electrode, Pt wire auxiliary electrode, and Ag/AgCl reference electrode at a scan rate of 100 mV/s with $TBAPF_6$ as the supporting electrolyte.

The electrochemical behavior of the mononuclear Fe^{III}(dpa) complex is quite different. This system shows a clearly reversible one-electron oxidation at almost the same potential as the Fe^{III}(ppq) complex, 0.01 V (ΔE_p = 76 mV). A second reversible oxidation is observed at 0.45 V (ΔE_p = 86 mV). These waves are thus assigned to the $Fe^{III/IV}$ and $Fe^{IV/V}$ couples. Both complexes show a reversible one-electron reduction. This reduction is most likely metal-based $Fe^{III} \rightarrow Fe^{II}$ and indicates that ppq in the dinuclear Fe^{III}(ppq) complex is a somewhat better electron acceptor than Fe^{III}(dpa).

The two complexes were also studied in pH 1 aqueous buffer where they both evidenced the onset of an electrocatalytic wave at about +1.25 V vs Ag/AgCl (Figure 3). The implication that

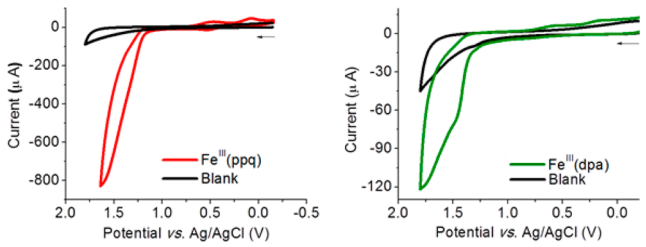

Figure 3. CV scans of Fe^{III} complexes (ppq, left and dpa, right) measured in pH 1 buffer with carbon working electrode, Pt wire auxiliary electrode, and Ag/AgCl reference electrode at a scan rate of 100 mV/s.

these complexes could serve as water oxidation catalysts prompted us to study their behavior in the presence of the strong chemical oxidant ceric ammonium nitrate (CAN). When CAN (0.1 M) was added to a nitric acid solution (pH 1) of either Fe^{III}(ppq) or Fe^{III}(dpa) (~2.5 μM), copious amounts of oxygen were generated immediately (Figure 4). It was also very clear that the dimeric ppq complex was considerably more active than the monomeric dpa complex. Interestingly, the ppq complex shows a fast initial rate (7920 h^{-1}) but looses most of its activity after 1 h, while the slower dpa complex continues to show activity after 1 h. The diminished activity of Fe^{III}(ppq) is apparently due to

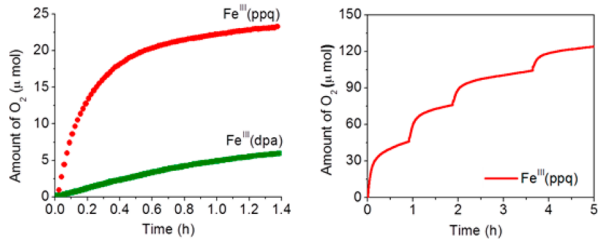

Figure 4. (Left) Plot of O_2 evolution vs time for Fe^{III}(ppq) (2.4 μM, red) and Fe^{III}(dpa) (2.5 μM, green) upon addition of CAN (0.1 M) in HNO_3 solution (10 mL, pH 1). (Right) The regeneration of O_2 evolution by addition of Fe^{III}(ppq) catalyst (50 μL of 1.29 mM solution) to 0.1 M HNO_3 (10 mL) containing CAN (0.1 M) and Fe^{III}(ppq) (10 μM) after O_2 evolution had diminished.

destruction of the catalyst, and activity can be restored by the addition of more catalyst (Figure 4).

The electrochemical and structural analysis of the two Fe complexes suggests that they might owe their catalytic activity to quite different mechanisms. An obvious question was whether the dimeric complex might dissociate to a monomeric species in solution. We examined the UV−vis spectra of both complexes in aqueous solution and saw no change after more than 6 h (Figure S2). We also studied the kinetics of the water oxidation process by measuring the amount of oxygen generated versus time for both Fe^{III}(ppq) and Fe^{III}(dpa) added to a CAN solution in nitric acid (Figure S3). From these plots we were able to measure initial rates, and when these rates were plotted against catalyst concentration, clear first order behavior was revealed (Figure 5). It appears most likely therefore that the dimeric catalyst remains intact during the oxidation process.

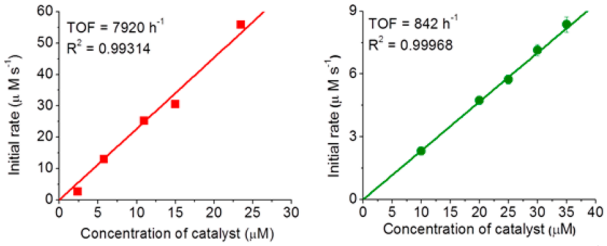

Figure 5. Initial rate of O_2 formation vs catalyst conc for Fe^{III}(ppq) (left) and Fe^{III}(dpa) (right).

In other related systems workers have reported the appearance of an absorption band at 613 nm that they attribute to the formation of a Fe^{V}=O species.[4] When we add CAN to an aqueous solution of Fe^{III}(ppq) we observe the immediate formation of a green color and band at 675 nm that quickly disappears after 6 min (Figure 6). To address the persistent concern about the possible formation of iron oxide nanoparticles, we have examined the reaction solutions for both Fe^{III}(ppq) and Fe^{III}(dpa) after the cessation of oxygen generation using dynamic light scattering. No evidence was found for the formation of any nanoparticles (Figure S4).

In conclusion, an alternate synthesis of the ppq ligand has been developed, and this ligand has been shown to react with $FeCl_3$ to form a μ-oxo bridged dimer. A similar mononuclear complex is formed with a bis-phenanthroline amine ligand (dpa) having the same square planar arrangement of its quaterpyridine-like backbone. It is suggested that steric encumbrance due to the *N*-isopentyl group of dpa may inhibit dimer formation. The ppq

DOI: 10.1021/jacs.5b08856
J. Am. Chem. Soc. 2015, 137, 13260−13263

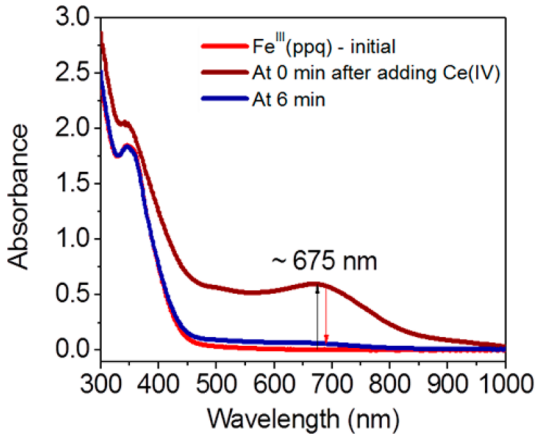

Figure 6. Electronic absorption spectrum of Fe^{III}(ppq) (0.1 mM, pH = 1) before and after treatment with 6 equiv of Ce^{IV}.

complex undergoes a two-electron oxidation that likely leads to a $Fe^{III}Fe^{V}$═O intermediate that subsequently oxidizes water with a TOF = 7920 h^{-1}. Future efforts will further examine the mechanism of the catalytic oxidation process, substituted derivatives of ppq, photochemical activation, and a possible macrocyclic analog of ppq.

■ ASSOCIATED CONTENT

Supporting Information

The Supporting Information is available free of charge on the ACS Publications website at DOI: 10.1021/jacs.5b08856.

Synthetic details and electrochemical data (PDF)
X-ray crystallographic data for Fe^{III}(ppq) CCDC 1407394 (CIF)
X-ray crystallographic data for Fe^{III}(dpa) CCDC 1407395 (CIF)

■ AUTHOR INFORMATION

Corresponding Author

*thummel@uh.edu

Notes

The authors declare no competing financial interest.

■ ACKNOWLEDGMENTS

This material is based upon work supported by the U.S. Department of Energy, Office of Science, Office of Basic Energy Sciences under award no. DE-FG02-07ER15888, the Advanced Light Source supported by the Director, Office of Science, Office of Basic Energy Sciences, of the U.S. Department of Energy under contract no. DE-AC02-05CH11231, and the Robert A. Welch Foundation (Grant E-621) for financial support of this work. We also thank Professor Karl Kadish for a helpful discussion, Ms. Maria A. Vorontsova for conducting dynamic light scattering experiments, and assistance from Dr. Andrew Kopecky.

■ REFERENCES

(1) (a) Zong, R.; Thummel, R. P. *J. Am. Chem. Soc.* **2005**, *127*, 12802−12803. (b) Tong, L.; Inge, A. K.; Duan, L.; Wang, L.; Zou, X.; Sun, L. *Inorg. Chem.* **2013**, *52*, 2505−2518. (c) Wasylenko, D. J.; Ganesamoorthy, C.; Koivisto, B. D.; Henderson, M. A.; Berlinguette, C. P. *Inorg. Chem.* **2010**, *49*, 2202−2209. (d) Tseng, H.-W.; Zong, R.; Muckerman, J. T.; Thummel, R. *Inorg. Chem.* **2008**, *47*, 11763−11773. (e) Zhang, G.; Zong, R.; Tseng, H.-W.; Thummel, R. P. *Inorg. Chem.* **2008**, *47*, 990−998. (f) Concepcion, J. J.; Jurss, J. W.; Brennaman, M. K.; Hoertz, P. G.; Patrocinio, A. O. T.; Iha, N. Y. M.; Templeton, J. L.; Meyer, T. J. *Acc. Chem. Res.* **2009**, *42*, 1954−1965. (g) Romain, S.; Vigara, L.; Llobet, A. *Acc. Chem. Res.* **2009**, *42*, 1944−1953.

(2) Hong, D.; Mandal, S.; Yamada, Y.; Lee, Y.-M.; Nam, W.; Llobet, A.; Fukuzumi, S. *Inorg. Chem.* **2013**, *52*, 9522−9531 and references contained therein..

(3) (a) Ellis, W. C.; McDaniel, N. D.; Bernhard, S.; Collins, T. J. *J. Am. Chem. Soc.* **2010**, *132*, 10990−10991. (b) Kundu, S.; Thompson, J. V.; Ryabov, A. D.; Collins, T. J. *J. Am. Chem. Soc.* **2011**, *133*, 18546−18549. (c) Chanda, A.; Shan, X.; Chakrabarti, M.; Ellis, W. C.; Popescu, D. L.; de Oliveira, F. T.; Wang, D.; Que, L., Jr.; Collins, T. J.; Münck, E.; Bominaar, E. L. *Inorg. Chem.* **2008**, *47*, 3669−3678.

(4) Panda, C.; Debgupta, J.; Díaz, D. D.; Singh, K. K.; Gupta, S. S.; Dhar, B. B. *J. Am. Chem. Soc.* **2014**, *136*, 12273−12282.

(5) To, W.-P.; Chow, T. W.-S.; Tse, C.-W.; Guan, X.; Huang, J.-S.; Che, C.-M. *Chem. Sci.* **2015**, *6*, 5891−5903.

(6) (a) Hoffert, W. A.; Mock, M. T.; Appel, A. M.; Yang, J. Y. *Eur. J. Inorg. Chem.* **2013**, *2013*, 3846−3857. (b) Connor, G. P.; Mayer, K. J.; Tribble, C. S.; McNamara, W. R. *Inorg. Chem.* **2014**, *53*, 5408−5410. (c) Chantarojsiri, T.; Sun, Y.; Long, J. R.; Chang, C. J. *Inorg. Chem.* **2015**, *54*, 5879−5887.

(7) (a) Coggins, M. K.; Zhang, M. T.; Vannucci, A. K.; Dares, C. J.; Meyer, T. J. *J. Am. Chem. Soc.* **2014**, *136*, 5531−5534. (b) Hong, D.; Mandal, S.; Yamada, Y.; Lee, Y. M.; Nam, W.; Llobet, A.; Fukuzumi, S. *Inorg. Chem.* **2013**, *52*, 9522−9531.

(8) (a) Fillol, J. L.; Codolà, Z.; Garcia-Bosch, I.; Gómez, L.; Pla, J. J.; Costas, M. *Nat. Chem.* **2011**, *3*, 807−813. (b) Codolà, Z.; Gómez, L.; Kieespies, S. T.; Que, L., Jr; Costas, M.; Fillol, J. L. *Nat. Commun.* **2015**, *6*, 5865.

(9) (a) Liu, Y.; Xiang, R.; Du, X.; Ding, Y.; Ma, B. *Chem. Commun.* **2014**, *50*, 12779−12782. (b) Ghosh, A.; Tiago de Oliveira, F.; Yano, T.; Nishioka, T.; Beach, E. S.; Kinoshita, I.; Münck, E.; Ryabov, A. D.; Horwitz, C. P.; Collins, T. J. *J. Am. Chem. Soc.* **2005**, *127*, 2505−2513.

(10) (a) Amini, M.; Najafpour, M. M.; Zare, M.; Holynskai, M.; Moghaddam, A. N.; Bagherzadeh, M. *J. Coord. Chem.* **2014**, *67*, 3026−3032. (b) Najafpour, M. M.; Moghaddam, A. N.; Sedigh, D. J.; Hołyńska, M. *Catal. Sci. Technol.* **2014**, *4*, 30−33.

(11) Chen, G.; Chen, L.; Ng, S.-M.; Man, W.-L.; Lau, T.-C. *Angew. Chem., Int. Ed.* **2013**, *52*, 1789−1791.

(12) Tong, L.; Zong, R.; Thummel, R. P. *J. Am. Chem. Soc.* **2014**, *136*, 4881−4884.

(13) Cottet, F.; Marull, M.; Lefebvre, O.; Schlosser, M. *Eur. J. Org. Chem.* **2003**, *2003*, 1559−1568.

(14) Mao, L.; Moriuchi, T.; Sakurai, H.; Fujii, H.; Hirao, T. *Tetrahedron Lett.* **2005**, *46*, 8419−8422.

(15) Bark, T.; Thummel, R. P. *Inorg. Chem.* **2005**, *44*, 8733−8739.

(16) Bianco, S.; Musetti, C.; Waldeck, A.; Sparapani, S.; Seitz, J. D.; Krapcho, A. P.; Palumbo, M.; Sissi, C. *Dalton Trans.* **2010**, *39*, 5833−5841.

(17) Bard, A. J.; Faulkner, L. R. *Electrochemical Methods: Fundamentals and Applications*, 2nd ed.; John Wiley & Sons, Inc.: New York, 2002.

DOI: 10.1021/jacs.5b08856
J. Am. Chem. Soc. 2015, 137, 13260−13263